AD-A087 797 NAVAL OCEAN SYSTEMS CENTER SAN DIEGO CA F/G 9/4
COMPARISON OF DETECTION PERFORMANCE OF SELECTED TWO-CHANNEL ALG--ETC(U)
SEP 79 D J EDELBLUTE, C L MELAND
UNCLASSIFIED NOSC/TD-328 NL

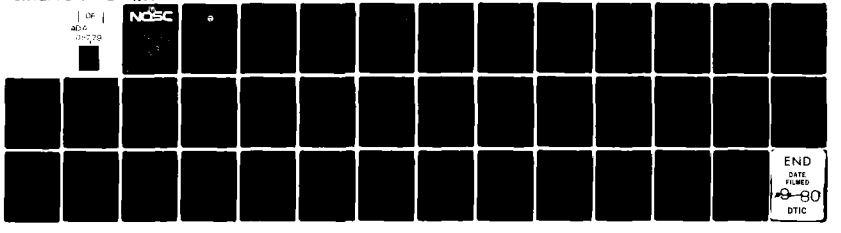

LEVEL II

12 B.S.

NOSC

NOSC TD 328

NOSC TD 328

Technical Document 328

COMPARISON OF DETECTION PERFORMANCE OF SELECTED TWO-CHANNEL ALGORITHMS

D. J. Edelblute
C. L. Meland

28 September 1979

Approved for public release; distribution unlimited

NAVAL OCEAN SYSTEMS CENTER
SAN DIEGO, CALIFORNIA 92152

NAVAL OCEAN SYSTEMS CENTER, SAN DIEGO, CA 92152

AN ACTIVITY OF THE NAVAL MATERIAL COMMAND

SL GUILLE, CAPT, USN
Commander

HL BLOOD
Technical Director

ADMINISTRATIVE INFORMATION

The work was conducted by personnel of the Analysis and Processing Branch, Systems Applications Division, by means of funding provided under program element 61152N, project ZR00001, task area ZR0110812, and work unit 711-ZS04.

Released by
T. F. Ball, Head
Systems Applications
Division

Under authority of
Dr. H. A. Schenck, Head
Undersea Surveillance
Department

UNCLASSIFIED

SECURITY CLASSIFICATION OF THIS PAGE *(When Data Entered)*

REPORT DOCUMENTATION PAGE

READ INSTRUCTIONS BEFORE COMPLETING FORM

1. REPORT NUMBER NOSC Technical Document 328 (TD 328)	2. GOVT ACCESSION NO. AD-A087797
3. RECIPIENT'S CATALOG NUMBER	
4. TITLE *(and Subtitle)* COMPARISON OF DETECTION PERFORMANCE OF SELECTED TWO-CHANNEL ALGORITHMS	5. TYPE OF REPORT & PERIOD COVERED Final Project Report
	6. PERFORMING ORG. REPORT NUMBER
7. AUTHOR(s) D. J. Edelblute C. L. Meland	8. CONTRACT OR GRANT NUMBER(s)
9. PERFORMING ORGANIZATION NAME AND ADDRESS Naval Ocean Systems Center San Diego, CA 92152	10. PROGRAM ELEMENT, PROJECT, TASK AREA & WORK UNIT NUMBERS 61152N, ZR00001, ZR0110812, 711-ZS04
11. CONTROLLING OFFICE NAME AND ADDRESS Naval Ocean Systems Center San Diego, CA 92152	12. REPORT DATE 28 September 1979
	13. NUMBER OF PAGES 36
14. MONITORING AGENCY NAME & ADDRESS *(if different from Controlling Office)*	15. SECURITY CLASS. *(of this report)* Unclassified
	15a. DECLASSIFICATION/DOWNGRADING SCHEDULE

16. DISTRIBUTION STATEMENT *(of this Report)*

Approved for public release; distribution unlimited

17. DISTRIBUTION STATEMENT *(of the abstract entered in Block 20, if different from Report)*

18. SUPPLEMENTARY NOTES

19. KEY WORDS *(Continue on reverse side if necessary and identify by block number)*

Interarray processing (IAP)
Two-channel algorithms
Data sequence correlation
Detection
Tracking

20. ABSTRACT *(Continue on reverse side if necessary and identify by block number)*

Recent work on intersensor processing has stimulated interest in techniques for determining information common to two data sequences which may be used for detection, tracking or a combination of these and other functions. Three algorithms which seemed naturally to suggest themselves for intersensor processing were compared. It was determined that the use of a normalization factor significantly degrades detection performance in regions characterized by low time-bandwidth product $TW \leq 64$. For $TW \geq 120$, all three algorithms performed about equally on the detection function. The principal implication of this work is that the operating mode of the system (which may dictate the low time-bandwidth product used) may affect the choice of algorithms to be used. In a

DD FORM 1 JAN 73 1473 EDITION OF 1 NOV 65 IS OBSOLETE
S/N 0102-LF-014-6601

UNCLASSIFIED

SECURITY CLASSIFICATION OF THIS PAGE *(When Data Entered)*

20. Continued.

tactical application where decisions must be made quickly, use of an unnormalized correlator may be mandatory. In a situation where long integration times are acceptable, a normalized formula such as the coherence detector may be chosen for data processing, as opposed to signal processing, economies.

CONTENTS

ILLUSTRATIONS

TABLES

TABLES (Continued)

INTRODUCTION

Recent work on interarray processing (IAP) has stimulated interest in techniques for correlating two data sequences. Such correlations may be used for detection or tracking or a combination of functions. This paper focuses on the detection function. The purpose of this study was to investigate the properties of three algorithms which seem naturally to suggest themselves for IAP. The first such algorithm simply correlates the two sequences. The other two algorithms normalize this value to a range from zero to one to form the familiar correlation coefficient or the coherence. To provide a baseline, all three were compared to the detection performance which would be achieved by using one array only, with the usual, simpler square law detection.

The increasing interest in IAP was one reason why such a study seemed appropriate. However, almost all IAP work to date has concentrated on one specific algorithm: the coherence detector. A major goal of this study was to open up the field to consideration of possible alternatives which might, in some cases, be advantageous.

Comparison of these algorithms is, however, a nontrivial problem for two reasons. First, each estimator has different statistical properties which are difficult to summarize. Second, the comparison can appear quite different for different sample sizes (or time-bandwidth products). Since assumed false-alarm probability, probability of detection, and integration time all affect the comparison, a fairly careful study was needed.

For such a study, some assumptions had to be made. The first was that the noise in both sequences was stationary, Gaussian, and uncorrelated between sequences. This assumption was tested by means of recorded ocean noise. The second assumption was that the signal was either a pure sinusoid (constant in the filtered data) or was a Gaussian process which differed from the noise only in amplitude and by its presence in both sequences. It was felt that these two assumptions should bracket the realistic cases. Both cases were analyzed. The third, and most questionable, assumption was that the signal-to-noise ratio in both sequences was the same. This assumption was made partly to simplify the problem to bring it within the scope of a 1-year effort, and partly because it is the most favorable case for comparison of IAP detection performance to single array performance.

The major results may be summarized as follows:

1. For time-bandwidth products less than about 64, the use of a normalization factor significantly degrades detection performance. In this region, even a square law detector operating on one array is likely to be superior. However, the unnormalized correlator performs well.
2. For time-bandwidth products greater than about 128, all three IAP algorithms perform about the same, so a selection among them can be made properly on criteria other than detection.
3. The results are not highly sensitive to the choice of a Gaussian or a steady-state signal assumption.
4. The tabulations and plots contained in this report should aid a system designer to estimate performance.

5. When tests were run by means of recorded ocean noise, the results were consistent with the theoretical predictions based on a Gaussian noise assumption.

The principal implication is that the operating mode of the system (which may dictate the time-bandwidth product used) may affect the choice of algorithm. In a tactical application where decisions must be made quickly, use of an unnormalized correlator may be mandatory. In a situation where long integration times are acceptable, a normalized formula such as the coherence detector may be chosen for display economy.

It should be noted that there are no significant differences in computational load or required computing speed between any of these algorithms. The "front end" of such a system would likewise be unaffected.

The subject is by no means exhausted. The results should eventually be extended to include the case of unequal signal-to-noise ratios in the two sequences. Field comparisons can also contribute significantly.

PROBLEM DEFINITION AND NOTATION

Let x(i) and y(i) denote the two data sequences. Since the discussion concerns narrowband data, both data sequences are assumed to be complex with zero mean. It is also assumed that any necessary time and/or frequency shifting has already been done to align the possible signals. Let $\overline{x^*x}$, $\overline{y^*y}$, and $\overline{x^*y}$ denote the second moments which are estimated by:

$$\langle x^*x \rangle = \frac{1}{K} \sum_{i=1}^{K} x^*(i)\, x(i)$$

$$\langle y^*y \rangle = \frac{1}{K} \sum_{i=1}^{K} y^*(i)\, y(i)$$

$$\langle x^*y \rangle = \frac{1}{K} \sum_{i=1}^{K} x^*(i)\, y(i).$$

where <quantity> denotes the estimator of the quantity.

It is assumed that samples from different times are independent, so that K is the true number of degrees of freedom in the estimator (ie, the time-bandwidth product).

Let s(i), $n_1(i)$, and $n_2(i)$ denote the signal, the noise in x(i), and the noise in y(i), respectively. The problem is to choose between the hypotheses:

H_0: $x(i) = n_1(i)$
$y(i) = n_2(i)$

H_1: $x(i) = s(i) + n_1(i)$
$y(i) = s(i) + n_2(i)$.

The following definitions and assumptions are made:

$$S = \overline{s^* s}$$

$$N = \overline{n_1^* n_1} = \overline{n_2^* n_2}$$

$$O = \overline{n_1^* n_2} = \overline{s^* n_1} = \overline{s^* n_2},$$

ie, the noises in the sequences are assumed independent and of equal power, and the signal is independent of all noise. Most importantly, n_1 and n_2 are assumed to be complex Gaussian random variables of zero mean.

A thresholding test procedure is to be used. That is, a test variable, t, will be computed from the second moments and compared with a predetermined threshold, T. (In some cases, T must be based on N.) The choice of t may vary with the application. Various optimality arguments, based on different assumptions, may give a variety of formulas for it. It is not the function of this project to sort out these arguments. Rather, the purpose here is to compare some natural choices on the basis of initial detection performance which is not necessarily the criterion under which the formula for t may be chosen.

The simplest detection procedure is to ignore the dual-sequence nature of the data, pick one sequence, and use a square law detector. Since this is the simplest and easiest technique, it will be used as a baseline against which the other techniques will be compared.

In this case, the test variable, t_1, is simply

$$t_1 = \langle x^* x \rangle,$$

and the test procedure is

$$t_1 = \langle x^* x \rangle \underset{H_0}{\overset{H_1}{\gtrless}} T_1 N.$$

A second obvious choice for t (suggested by certain matched filter arguments) is to correlate the two sequences. Here the test procedure is

$$t_2 = \mathrm{Re}\, \langle x^* y \rangle \underset{H_0}{\overset{H_1}{\gtrless}} T_2 N.$$

Since this formula uses information from both sequences, it seems intuitively that it should perform better than t_1. This will be shown to be the case, although it should be remembered that this assumes an equal signal-to-noise ratio in both sequences.

Although both of the above formulas perform fairly well, as will be shown, the determination of the threshold depends on a prior estimate of the noise level, N. Usually there are various ways this can be done. However, this requirement can be removed by the normalization used in calculation of correlation coefficients. In this case, the test procedure is

$$t_3 = \frac{\mathrm{Re}\,\langle x^*y\rangle}{\sqrt{\langle x^*x\rangle\,\langle y^*y\rangle}} \underset{H_0}{\overset{H_1}{\gtrless}} T_3.$$

Here, T_3 can be computed simply as a function of false-alarm rate.

Concern for phase uncertainties in the signal has led some people to use a slightly more robust formula:

$$t_4 = \frac{|\langle x^*y\rangle|^2}{\langle x^*x\rangle\,\langle y^*y\rangle} \underset{H_0}{\overset{H_1}{\gtrless}} T_4.$$

These options are illustrated in figure 1. As can be seen, most of the computational effort is expended in computing the estimated second moments, $\langle x^*x\rangle$, $\langle y^*y\rangle$, and $\langle x^*y\rangle$. Thus there is little to choose from when comparing the computational load of one formula versus another (except for $t_1 = \langle x^*x\rangle$).

It should be noted that one of the formulas, $\langle (x+y)^*(x+y)\rangle$ is not analyzed. This is because it does not constitute a separate case. It is a power estimator and therefore has the same statistical properties as $\langle x^*x\rangle$. It simply has a 3-dB improvement in signal-to-noise ratio. Thus whatever detection performance is achieved with $\langle x^*x\rangle$ is achieved with a 3-dB lower input signal-to-noise ratio using $\langle (x+y)^*(x+y)\rangle$.

The central problem is to compare the detection performances of t_1, t_2, t_3, and t_4. This is complicated by the fact that each test variable has different distributional properties (eg, the relationship between false-alarm probability and threshold) and different relationship to the input parameters.

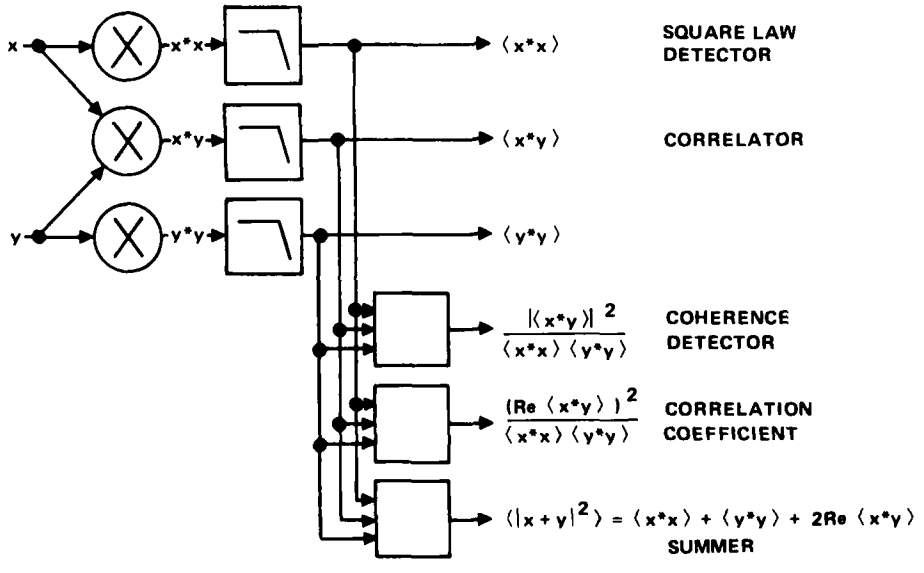

Figure 1. Two-channel detector structures.

Comparisons of this sort are sometimes made by using receiver operating characteristics (ROC) curves, which are plots of probability of detection, P_d, versus false-alarm probability, P_f (see reference 1). This approach is unsatisfactory here because:

1. Each curve describes only one set of processing parameters (signal-to-noise ratio and integration time) and an inordinate number of such curves would be required.
2. ROC curves tend to be too sensitive. In the key cases, the values of P_d and P_f change very fast relative to fairly small changes in signal strength or time-bandwidth product.

A somewhat more instructive approach is to plot false-alarm probability, P_f, versus threshold. However, the relationship between threshold and other important parameters is not obvious, so the value of such plots seems limited. But the threshold does have significance in terms of the signal strength, or signal-to-noise ratio, which will trigger the detector. To see how this works, consider for each detector the case where the signal strength is marginally enough to trigger the detector.

For the square law detector,

$$t_1 = \overline{x^* x} = T_1 N \quad \text{or}$$

$$(s + n_1)^* (s + n_1) = T_1 N$$

$$S + N = T_1 N$$

$$S/N + 1 = T_1.$$

For the correlator,

$$t_2 = \mathrm{Re}\, \overline{x^* y} = T_2 N \quad \text{or}$$

$$(s + n_1)^* (s + n_2) = T_2 N$$

$$S = T_2 N$$

$$S/N = T_2.$$

For the normalized formulas, it is convenient to be a little careless about the averaging process. This will introduce a bias in the formulas, but it will later be shown to be unimportant. Actually, because of asymmetries in the distributions, all of the formulas contain biases which will be shown to be small and unimportant.

For the correlation coefficient,

$$t_3 = \frac{\mathrm{Re}\, \overline{x^* y}}{\sqrt{\overline{\langle x^* x \rangle}\, \overline{\langle y^* y \rangle}}} = T_3$$

1. Van Trees, H. L., Detection, Estimation and Modulation Theory, Part I, John Wiley and Sons, Inc., 1968.

$$\frac{\overline{(s+n_1)^*(s+n_2)}}{\sqrt{\overline{(s+n_1)^*(s+n_1)}\;\overline{(s+n_2)^*(s+n_2)}}} = T_3$$

$$\frac{S}{\sqrt{(S+N)(S+N)}} = T_3$$

$$\frac{(S/N)}{(S/N+1)} = T_3.$$

In a similar manner, for the coherence detector,

$$t_4 = \frac{|\overline{x^*y}|^2}{\overline{x^*x}\;\overline{y^*y}} = T_4$$

$$\frac{|\overline{(s+n_1)(s+n_2)}|^2}{\overline{(s+n_1)^*(s+n_1)}\;\overline{(s+n_1)^*(s+n_2)}} = T_4$$

$$\frac{S^2}{(S+N)^2} = T_4$$

$$\frac{(S/N)^2}{(S/N+1)^2} = T_4.$$

Thus each threshold can be expressed in terms of a signal-to-noise ratio which must be exceeded for reliable detection. This will be called the threshold signal-to-noise ratio (TSNR). So, instead of plotting false-alarm probability versus threshold, the false-alarm probability will be plotted as a function of TSNR. Thus plots of false-alarm rate versus TSNR can be directly compared for each algorithm. As a side issue, the t_2 and t_3 test variables assume both positive and negative values, whereas the other test variables are positive. For this reason, the plotted P_f for t_2 and t_3 are "two-sided"; that is, they indicate the probability that the magnitude of the test variable will exceed the threshold on the positive or negative side. As is apparent in the figures, this has a very small effect on the result because of the small slope of the curves for P_f of any practical interest.

These plots, figures 2, 3, 4, and 5, form the primary result of this study. Figure 6 displays the TSNR for the algorithms under consideration as a function of P_F for three selected time bandwidth products which span the region of most applications. It illustrates where the algorithms differ and where the differences become negligible. The rest of this paper is concerned with how these plots were derived, what changes would result from slight variations in assumptions (ie, how representative of actual situations these results are likely to be) and what the implications are.

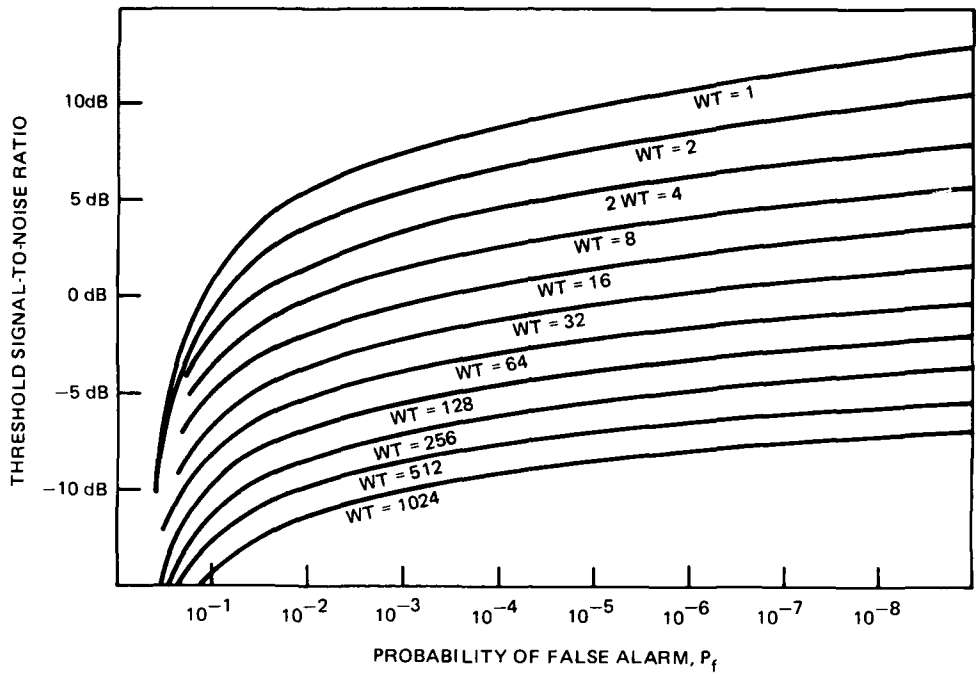

Figure 2. Square law detector.

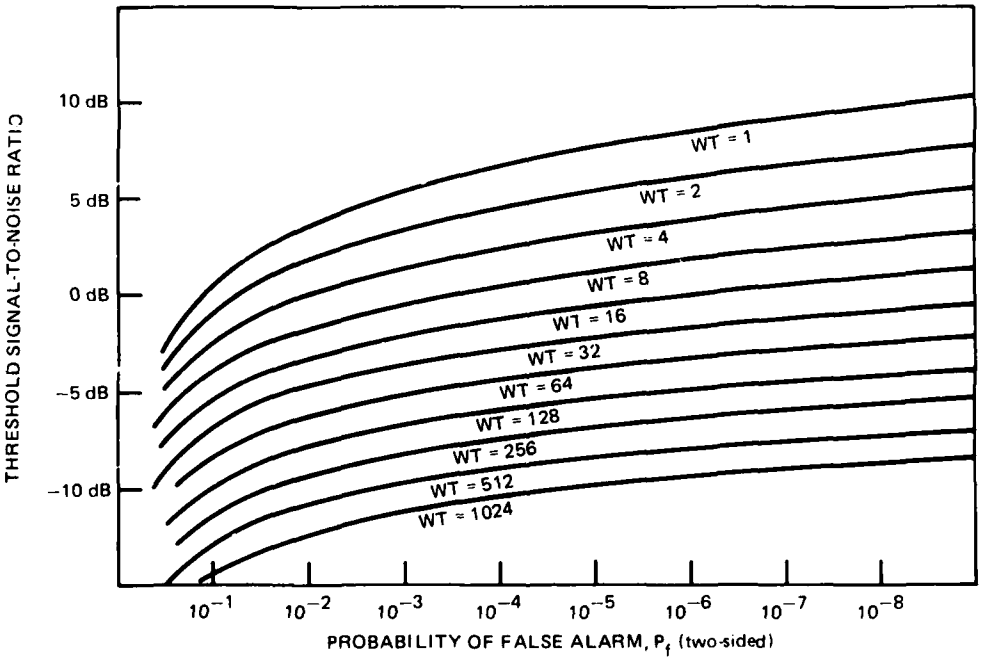

Figure 3. Correlator.

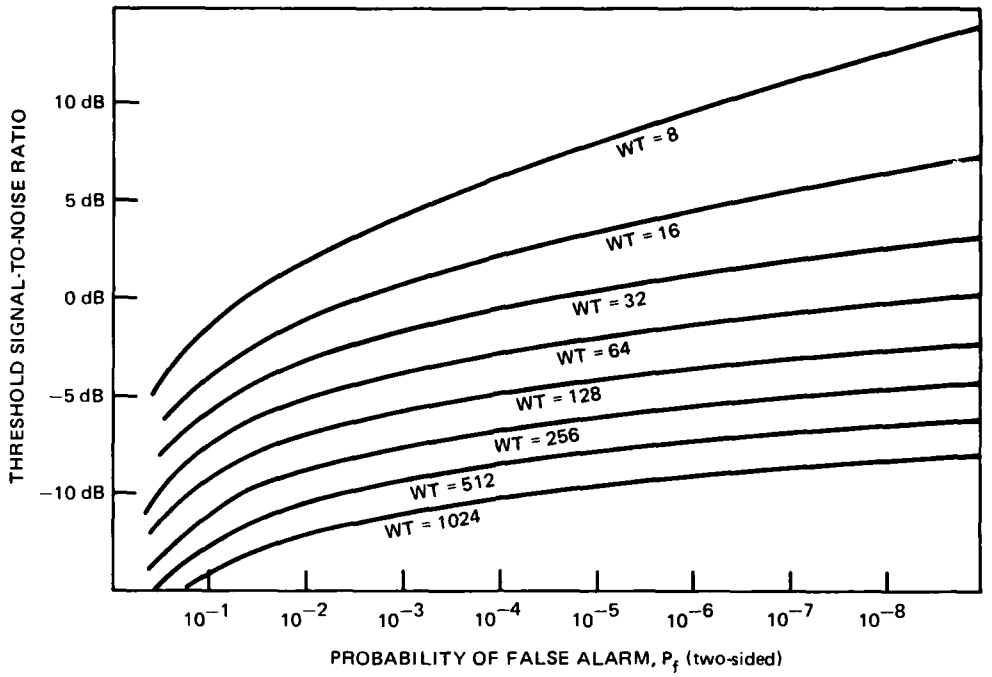

Figure 4. Correlation coefficient.

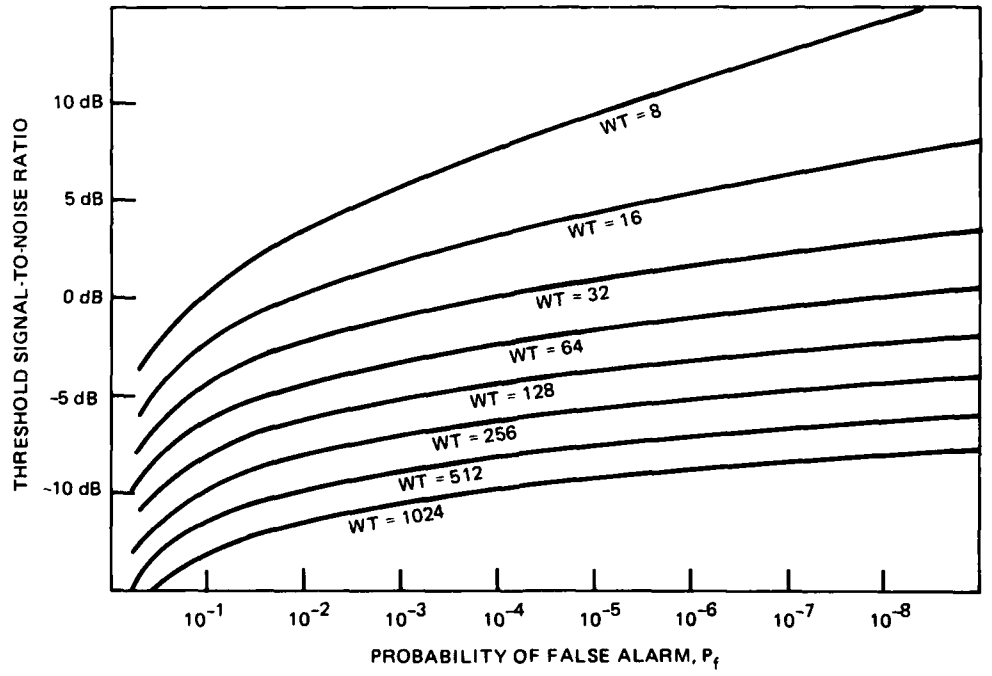

Figure 5. Coherence detector.

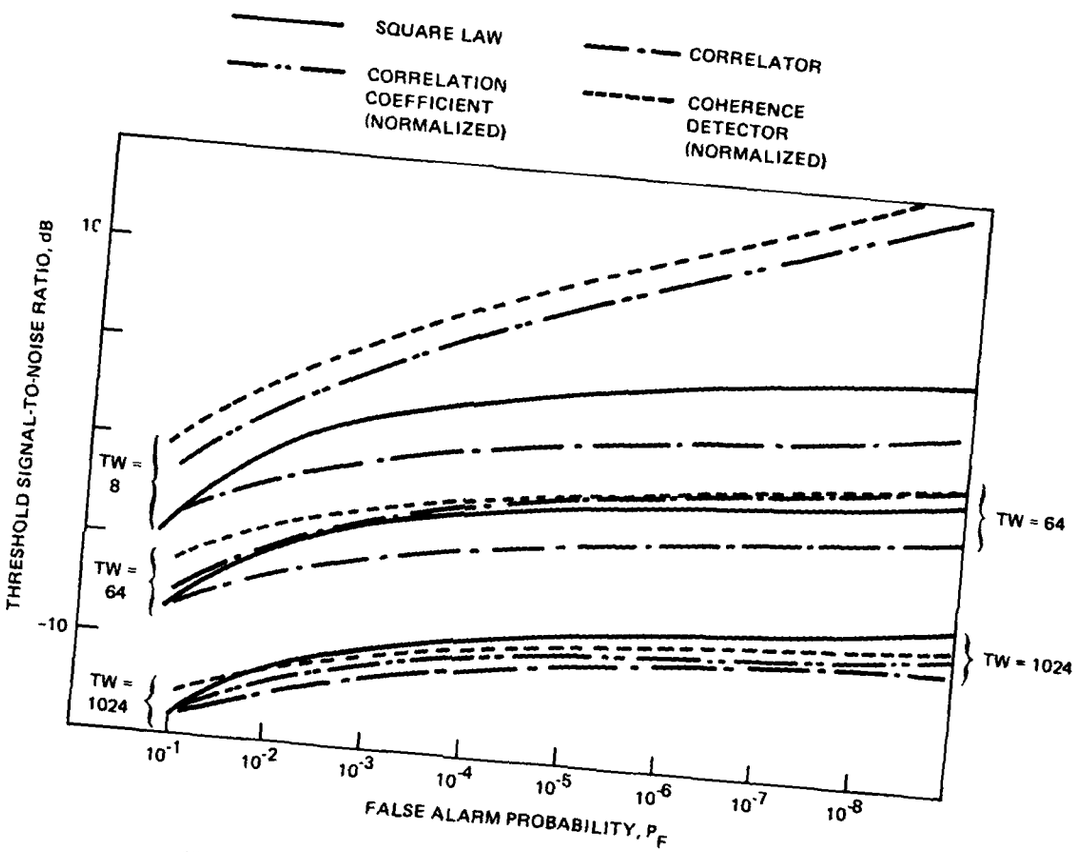

Figure 6. Threshold signal-to-noise ratio at algorithm output.

THEORY

The first problem is to derive the false-alarm probability equation for each process. Recall that these deviations all assume that S = 0, and that n_1 and n_2 are independent complex random variables with zero means and equal variances, $n_1^* n_1 = n_2^* n_2 = N$. The equations will give the false-alarm rate, P_f, in terms of the thresholds, T_1, T_2, T_3, and T_4. However, the plots will be done in terms of the threshold signal-to-noise ratios. As noted above, these are connected to T_1, T_2, T_3, and T_4, by

$$(S/N)_1 = T_1 - 1$$

$$(S/N)_2 = T_2$$

$$(S/N)_3 = T_3/(1 - T_3)$$

$$(S/N)_4 = \sqrt{T_4}/(1 - \sqrt{T_4}).$$

SQUARE LAW DETECTOR

For the square law detector, the theory is especially well known. Since n_1 is composed of a real part and an imaginary part, $|n_1|$ is a Raleigh variable. Then $n_1^* n_1$ has an exponential distribution. Let $u_1 = x_1^* x_1 = n_1^* n_1$, $f_1(u)$ denote the probability density function of u_1, and $F_1(u)$ denote the cumulative probability function of u. Then

$$f_1(u_1) = \frac{1}{N} \exp(-u_1/N).$$

Since the test variable is

$$t_1 = \frac{1}{K}[u_1(1) + u_1(2) + \cdots + u_1(K)],$$

the probability density function of t_1 can be obtained by repeated convolutions of the $f_1(u_1)$. This results in a Gamma distribution:

$$f_1(t_1, K) = \frac{(K/N)\,(Kt_1/N)^{K-1} \exp(-K\,t_1/N)}{(K-1)!}.$$

So, for the square law detector

$$P_F(T_1) = \int_{T_1 N}^{\infty} f_1(t, K)\, dt$$

$$= \frac{1}{(K-1)!} \int_{T_1 N}^{\infty} (Kt_1/N)^{K-1} \exp(-Kt_1/N)\,(K/N)\, dt_1$$

$$= \frac{\Gamma(K, KT_1 N/N)}{\Gamma(K)} = \frac{\Gamma(K, KT_1)}{\Gamma(K)}$$

where $\Gamma(K, KT_1)$ and $\Gamma(K)$ are the incomplete gamma function and the gamma function, respectively. For the purposes of this discussion, they are characterized by the relationships

$$\Gamma(K) = (K - 1)!$$

and

$$\Gamma(K + 1, u) = K\Gamma(K, u) + u^K \exp(-u).$$

CORRELATOR

The theory for the correlator is less well known and somewhat more difficult to derive. It is convenient to convert the problem to one involving real variables by letting $n_1 = nr_1 + \sqrt{-1}\, ni_1$ and $n_2 = nr_2 + \sqrt{-1}\, ni_2$. Therefore, $\mathrm{Re}(n_1^* n_2) = nr_1\, nr_2 + ni_1 ni_2$. Since, for Gaussian distributions, the real and imaginary parts of a variable are independent, the process of averaging the real part of K complex products is the same as averaging 2K real products.

First, let u and v denote two independent, zero mean, Gaussian random variables. So

$$\overline{uv} = 0$$
$$\overline{u^2} = \sigma_1^2$$
$$\overline{v^2} = \sigma_2^2.$$

The joint distribution function is

$$f(u, v) = \frac{1}{2\pi\sigma_1\sigma_2} \exp\left\{\frac{-u^2/\sigma_1^2 - v^2/\sigma_2^2}{2}\right\}.$$

Now if $w = uv$, the distribution function for w becomes

$$f(w) = \int_{-\infty}^{\infty} \left|\frac{1}{v}\right| f(w/v, v)\, dv$$

$$= \frac{1}{2\pi\sigma_1\sigma_2} \int_{-\infty}^{\infty} \left|\frac{1}{v}\right| \exp\left\{\left(\frac{-1}{2}\right)\left(\frac{w^2}{v^2\sigma_1^2} + \frac{v^2}{\sigma_2^2}\right)\right\} dv$$

$$= \frac{1}{\pi\sigma_1\sigma_2} \int_0^{\infty} \left|\frac{1}{v}\right| \exp\left\{\frac{-v^2}{2\sigma_2^2} - \frac{w^2}{2\sigma_1^2 v^2}\right\} dv$$

$$= \frac{1}{\pi\sigma_1\sigma_2} K_0\left(\frac{w}{\sigma_1\sigma_2}\right)$$

where K_0 is a Bessel function of an imaginary argument.

Since the test variable is computed by averaging 2K different values of w, the obvious procedure is to use repeated convolutions of K_0 with itself. However, it seems easier to use Fourier transforms.

$$F\{f(w)\} = \frac{1}{\pi\sigma_1\sigma_2}\int_{-\infty}^{\infty} \exp(-\sqrt{-1}\,\omega w)\, K_0\left(\frac{w}{\sigma_1\sigma_2}\right) dw$$

$$= \frac{1}{\sqrt{1 + (\omega\sigma_1\sigma_2)^2}}.$$

So if $W = w_1 + w_2 + \cdots + w_{2K}$, then

$$F\{f(W)\} = \left(\frac{1}{1 + (\omega\sigma_1\sigma_2)^2}\right)^K$$

$$f(W) = \frac{1}{2\pi}\int_{-\infty}^{\infty} \left(\frac{1}{1 + (\omega\sigma_1\sigma_2)^2}\right)^K \exp(\sqrt{-1}\,\omega W)\, d\omega$$

$$= \frac{1}{\pi\sigma_1\sigma_2}\int_0^{\infty} \frac{\cos|\omega W/(\sigma_1\sigma_2)|}{(1 + \omega^2)^K}\, d\omega$$

$$= \frac{\exp[-W/(\sigma_1\sigma_2)]}{\sigma_1\sigma_2\, 2^{2K-1}\,(K-1)!} \sum_{i=0}^{K-1} \frac{(2K-i-2)!\,[2W/(\sigma_1\sigma_2)]^i}{i!\,(K-i-1)!}.$$

So

$$P_F = \frac{1}{2^{2K-1}\,(K-1)!\,\sigma_1\sigma_2} \sum_{i=0}^{K-1} \frac{(2K-i-2)!\,2^i}{i!\,(K-i-1)!} \int_{KNT_2}^{\infty} \left(\frac{W}{\sigma_1\sigma_2}\right)^i \exp\left(\frac{-W}{\sigma_1\sigma_2}\right) dW$$

$$= \frac{1}{2^{2K-1}\,(K-1)!} \sum_{i=1}^{K-1} \frac{(2K-i-2)!\,2^i}{i!\,(K-i-1)!}\,\Gamma(i+1, KNT_2/\sigma_1\sigma_2).$$

Note that under the above assumptions $\sigma_1\sigma_2 = \sigma_1^2 = \sigma_2^2 = N/2$, so $KNT_2/(\sigma_1\sigma_2) = 2KT_2$.

$$P_F(T_2) = \frac{1}{2^{2K-1}\,(K-1)!} \sum_{i=1}^{K-1} \frac{(2K-i-2)!\,2^i}{i!\,(K-i-1)!}\,\Gamma(i+1, 2KT_2).$$

CORRELATION COEFFICIENT

The distribution of the correlation coefficient is well known and documented once the problem has been translated from complex variables to real variables, as was done in the derivation for the correlator. Again, note that

$$\mathrm{Re}\,\langle x^* y\rangle = \frac{1}{K}[\,xr(1)\,yr(1) + xi(1)\,yi(1) + \cdots + xr(K)\,yr(K) + xi(K)\,yi(K)],$$

$$\langle x^* x\rangle = \frac{1}{K}[\,xr^2(1) + xi^2(1) + \cdots + xr^2(K) + xi^2(K)]$$

$$\langle y^* y\rangle = \frac{1}{K}[\,yr^2(1) + yi^2(1) + \cdots + yr^2(K) + yi^2(K)].$$

So t_3 looks like the result of an ordinary estimated correlation coefficient from 2K real variables. Mood and Graybill (reference 2) give

$$f(\hat{\rho}) = \frac{[(2K-3)/2]!\,(1-\hat{\rho}^2)^{(2K-4)/2}}{\sqrt{\pi}\,[(2K-4)/2]!}.$$

However, this is for the case in which the true mean value is unknown. Since the variables were known to be zero mean, the number of degrees of freedom was increased by one. (This was suggested by Dr. R. Riffenburgh, NOSC.) Thus the formula used was

$$P_F(T_3) = \frac{(K-1)!}{\sqrt{\pi}\left(\frac{2K-3}{2}\right)!}\int_{T_3}^{1}(1-t^2)^{\frac{2K-3}{2}}\,dt.$$

This formula, if integrated analytically, leads to a very cumbersome expression. However, it lends itself to numerical integration. The values plotted were computed by numerical integration.

COHERENCE DETECTOR

The deviation involved in the false-alarm probability for the coherence detector is rather involved. However, Goodman (reference 3) has shown that

$$P_F(T_4) = (1-T_4)^{K-1}.$$

2. Mood, A. M., and F. A. Graybill, Introduction to the Theory of Statistics, McGraw-Hill, 1963.
3. Goodman, N. R., On the Joint Estimation of the Spectra, Cospectrum, and Quadrature Spectrum of a Two-Dimensional Stationary Gaussian Process, New York University, Engineering Statistics Laboratory, March 1957.

DISCUSSION

These formulas were used to compute the values plotted in figures 2, 3, 4, and 5. They constitute the major results of this report. However, before they can be taken at face value, two questions must be addressed:

1. How closely does ocean noise correspond to the results which are based on Gaussian input assumptions?
2. Does consideration of the signal plus noise distributions change the results significantly, especially if a probability of detection other than 0.5 is used?

COMPARISON WITH EXPERIMENTAL DATA

The first issue to be addressed is the accuracy with which the theoretical results predict performance on actual data. For this purpose, recordings from the DARPA Fixed/Mobile Experiment were used. Data sequences were chosen which were known to contain no common signal. From these, Mr. L. Schilling of NOSC computed sets of test variables for the normalized functions; ie, the correlation coefficient and the coherence detector. For each set, a cumulative distribution function was computed. Since the cumulative distribution function is one minus the false-alarm probability, a false-alarm probability for each set could be tabulated. Thus several dozen tabulations of false-alarm probability versus threshold signal-to-noise ratio were generated.

Each tabulation represents the number of false alarms encountered in a set of 16,384 test values. However, the number of independent values is not known and is probably much smaller than 16,384. This lack of knowledge of the precise number of independent values, or degrees of freedom, is a minor problem in interpreting the results.

The most thorough comparisons were done for the case of WT = 8. Although this time-bandwidth product is somewhat small for serious detection processing, it seems a reasonable choice for statistical testing of this sort.

For each tabulation, a comparison with the theoretical values (in figures 4 and 5) had to be made. These comparisons needed to be quantitative and the set of all comparisons had to be summarized. The solution chosen was to use the maximum absolute difference between the theoretical and the observed false-alarm counts. These comparisons are shown in table 1. Each value shows the largest absolute difference between the theoretical false-alarm probability and the observed false-alarm probability for one set of 16,384 values of t_3 and t_4. To facilitate the comparisons, the signs have been preserved. A positive sign (+) means that the greatest separation between theoretical and actual curves occurred at a point where the observed curve ran below the theoretical curve. Thus, for the first entry, the largest difference in false-alarm rate was 0.8% at a point where the observed false-alarm rate was below the theoretical value. A mixed sign (±) indicates that this difference occurred two or more times, and that the observed curve was above the theoretical for one of these values and below for the other.

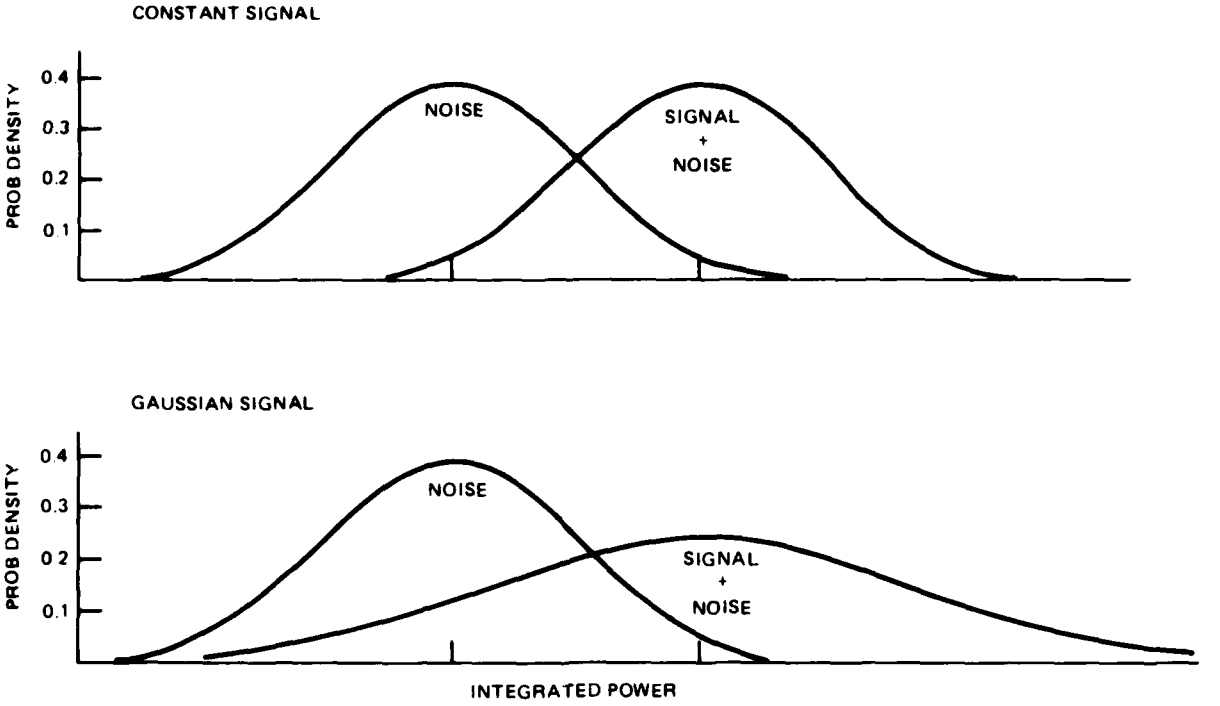

Figure 7. Alternate signal assumptions.

The tabulated differences in table 1 show no obvious pattern. This, plus the fact that they are small (never more than 3%), seems to indicate that the theoretical curves give as good a prediction of the actual false-alarm probability as reasonably could be expected.

Unfortunately, because the number of independent values in each set of 16,384 points is unknown, a precise use of the Kolmogorov-Smirnov test is not possible. However, the overall agreement of theory and observation appears excellent.

The principal difficulty in dealing with the signal plus noise distribution considerations is the number of special cases which must be considered. The effort here will be to bracket the major alternatives.

The first problem is to characterize the signal. There are two major alternatives. The signal can be a Gaussian random process like the noise, or it can be a constant which is added to the noise. The difference is illustrated in figure 7. For a constant signal, the distribution of (x^*x) is simply moved to the right. For a Gaussian signal, not only is the distribution moved to the right, but the variance of the signal is added to the variance of the noise. This difference may be unimportant when a 0.5 probability of detection is used, but may make a noticeable difference if a higher or lower probability is used. For instance, a 0.1 probability of detection would occur with a weaker signal under the Gaussian signal hypothesis than under the constant signal hypothesis. However, to achieve a probability of detection of 0.9 requires a stronger signal under the Gaussian signal hypothesis.

Correlation Coefficient	Coherence Detector
+0.008	-0.030
-0.008	+0.030
+0.006	+0.015
-0.005	+0.002
+0.013	-0.017
-0.007	-0.020
+0.004	+0.016
+0.014	-0.016
-0.020	+0.010
-0.004	-0.020
-0.004	+0.010
-0.012	-0.008
+0.011	-0.018
+0.006	-0.008
+0.010	+0.012
+0.010	-0.004
-0.004	-0.015
+0.009	+0.008
-0.003	-0.011
-0.008	+0.017
+0.010	±0.007
+0.010	+0.013
+0.008	+0.011
-0.003	-0.025
-0.006	±0.013
-0.018	-0.014
	+0.017
	±0.005
	+0.012
	+0.013
	+0.006
	-0.014
	-0.011
	+0.006
	-0.015
	-0.017
	-0.013
	-0.015
	-0.021
	-0.021
	-0.006
	+0.013
	+0.013
	-0.014
	+0.008
	+0.015

Table 1. False-alarm probability differences, WT = 8 (theory-observed).

The constant signal case might arise, for instance, if the bandwidth of the signal is much narrower than the analysis bandwidth which was used to produce the narrowband data sequences. The Gaussian signal case may arise when the signal bandwidth nearly matches the analysis bandwidth.

The principal assumption with respect to this issue is that these two cases, Gaussian signal and constant signal, bracket the important real-world cases.

Since, for the signal plus noise distributions, the probabilities of interest are limited to roughly 0.05 to 0.95, it was possible to obtain the probability curves with reasonable accuracy by means of Monte Carlo simulations. (Such an approach would not have worked well for the false-alarm probability curves because of the large number of trials necessary to verify false-alarm probabilities of 10^{-8} or 10^{-10}.) This was fortunate because the theoretical functions are substantially more cumbersome than for the noise-only cases.

A fairly extensive set of Monte Carlo simulations was run for various input signal-to-noise ratios. In each case, probability of detection was tabulated as a function of threshold signal-to-noise ratio. From these tabulations, tables 2 to 9 were compiled. For various false-alarm probabilities, they show what input signal-to-noise ratio would be required for probabilities of detection of 0.1, 0.5, and 0.9.

From these, various other tables and plots were obtained, as will be described in the next section.

Square Law Detector - Gaussian Signal

Input SNR (dB)	TSNR P_D (90%)	TSNR P_D (50%)	TSNR P_D (10%)	Input SNR (dB)	TSNR P_D (90%)	TSNR P_D (50%)	TSNR P_D (10%)
WT = 2				WT = 16			
-5		-9.2	1.9	-5		-5.4	-1.2
-4		-7.3	2.4	-4		-4.4	-0.6
-3		-5.6	2.9	-3		-3.3	0.0
-2		-4.3	3.4	-2	-8.6	-2.3	0.7
-1		-2.9	4.0	-1	-6.0	-1.2	1.4
0		-1.6	4.6	0	-4.0	-0.2	2.2
1		-0.5	5.3	1	-2.4	0.8	3.1
2		0.7	6.1	2	-0.9	1.9	3.9
3		1.8	6.9	3	0.4	2.9	4.8
4		2.9	7.7	4	1.6	3.9	5.7
5		4.0	8.5	5	2.8	4.9	6.6
WT = 4				WT = 32			
-5		-6.4	0.8	-5		-5.2	-2.0
-4		-5.1	1.3	-4		-4.1	-1.4
-3		-3.9	1.8	-3	-7.6	-3.1	-0.7
-2		-2.8	2.4	-2	-5.7	-2.1	0.1
-1		-1.7	3.0	-1	-4.0	-1.1	0.9
0		-0.6	3.7	0	-2.5	-0.1	1.7
1		0.4	4.5	1	-1.2	0.9	2.5
2	-8.6	1.4	5.3	2	0.1	2.0	3.4
3	-5.2	2.5	6.1	3	1.2	3.0	4.3
4	-2.8	3.5	6.9	4	2.4	4.0	5.2
5	-0.9	4.5	7.8	5	3.5	5.0	6.2
WT = 8				WT = 64			
-5		-5.8	-0.3	-5	-9.7	-5.1	-2.8
-4		-4.6	0.2	-4	-7.5	-4.1	-2.1
-3		-3.5	0.8	-3	-5.8	-3.0	-1.3
-2		-2.4	1.5	-2	-4.3	-2.0	-0.5
-1		-1.4	2.2	-1	-2.9	-1.0	0.4
0	-7.7	-0.3	2.9	0	-1.6	0.0	1.2
1	-5.1	0.7	3.7	1	-0.4	1.0	2.1
2	-3.1	1.7	4.5	2	0.7	2.0	3.0
3	-1.3	2.8	5.4	3	1.8	3.0	4.0
4	0.1	3.8	6.2	4	2.9	4.0	4.9
5	1.5	4.8	7.1	5	4.0	5.0	5.8

Table 2. P_D as a function of TW and TSNR.

Square Law Detector Constant Signal

Input SNR (dB)	TSNR P_D (90%)	TSNR P_D (50%)	TSNR P_D (10%)	Input SNR (dB)	TSNR P_D (90%)	TSNR P_D (50%)	TSNR P_D (10%)
WT = 2				WT = 16			
-5		-9.4	1.8	-5		-5.4	-1.3
-4		-7.2	2.2	-4		-4.3	-0.7
-3		-5.4	2.6	-3		-3.3	-0.1
-2		-3.9	3.1	-2	-7.6	-2.2	0.5
-1		-2.5	3.6	-1	-5.2	-1.2	1.3
0		-1.2	4.2	0	-3.3	-0.1	2.0
1		0.1	4.8	1	-1.7	0.9	2.8
2		1.3	5.4	2	-0.2	1.9	3.5
3	-8.1	2.4	6.1	3	1.2	2.9	4.4
4	-3.3	3.5	6.8	4	2.4	4.0	5.2
5	-0.5	4.6	7.5	5	3.7	5.0	6.1
WT = 4				WT = 32			
-5		-6.6	0.7	-5		-5.1	-2.1
-4		-5.3	1.2	-4	-10.0	-4.1	-1.5
-3		-4.0	1.6	-3	-7.3	-3.1	-0.8
-2		-2.8	2.2	-2	-5.3	-2.1	-0.1
-1		-1.6	2.7	-1	-3.6	-1.1	0.7
0		-0.5	3.4	0	-2.1	0.0	1.5
1	-8.0	0.6	4.0	1	-0.7	1.0	2.3
2	-4.2	1.7	4.7	2	0.6	2.0	3.1
3	-1.8	2.8	5.4	3	1.8	3.0	4.0
4	0.2	3.8	6.2	4	2.9	4.0	4.9
5	1.9	4.8	7.0	5	4.1	5.0	5.8
WT = 8				WT = 64			
-5		-5.7	-0.4	-5	-9.3	-5.1	-2.8
-4		-4.6	0.1	-4	-7.2	-4.1	-2.1
-3		-3.5	0.7	-3	-5.5	-3.0	-1.4
-2		-2.4	1.3	-2	-4.0	-2.0	-0.6
-1	-9.3	-1.3	1.9	-1	-2.6	-1.0	0.2
0	-5.7	-0.5	2.6	0	-1.4	0.0	1.1
1	-3.3	0.8	3.3	1	-0.2	1.0	1.9
2	-1.4	1.8	4.0	2	1.0	2.0	2.8
3	0.2	2.9	4.8	3	2.2	3.0	3.7
4	1.7	3.9	5.6	4	3.3	4.0	4.7
5	3.0	4.9	6.5	5	4.3	5.0	5.6

Table 3. P_D as a function of TW and TSNR.

Correlator Gaussian Signal

Input SNR (dB)	TSNR P_D (90%)	TSNR P_D (50%)	TSNR P_D (10%)	Input SNR (dB)	TSNR P_D (90%)	TSNR P_D (50%)	TSNR P_D (10%)
WT = 2				WT = 16			
-5		-3.9	0.8	-5		-5.1	-2.0
-4		-3.5	1.3	-4		-4.1	-1.3
-3		-3.0	1.8	-3	-8.1	-3.1	-0.6
-2		-2.4	2.4	-2	-6.1	-2.1	0.2
-1	-9.6	-1.7	3.1	-1	-4.4	-1.1	1.0
0	-8.8	-0.8	3.9	0	-3.0	-0.1	1.9
1	-7.9	0.1	4.7	1	-1.6	0.9	2.7
2	-6.9	1.0	5.5	2	-0.4	1.9	3.6
3	-5.8	2.0	6.4	3	0.4	2.9	4.6
4	-4.5	3.1	7.3	4	1.9	3.9	5.5
5	-3.2	4.1	8.2	5	3.1	4.9	6.4
WT = 4				WT = 32			
-5		-4.6	-0.3	-5	-9.6	-5.1	-2.7
-4		-4.0	0.2	-4	-7.7	-4.1	-1.9
-3		-3.3	0.9	-3	-5.9	-3.1	-1.2
-2	-10.0	-2.4	1.6	-2	-4.5	-2.1	-0.4
-1	-8.8	-1.5	2.3	-1	-3.1	-1.1	0.5
0	-7.2	-0.5	3.1	0	-1.9	0.0	1.4
1	-5.8	0.5	3.9	1	-0.7	1.0	2.3
2	-4.2	1.5	4.8	2	0.4	2.0	3.2
3	-2.6	2.6	5.7	3	1.6	3.0	4.2
4	-1.1	3.6	6.6	4	2.6	4.0	5.1
5	0.2	4.6	7.5	5	3.7	5.0	6.1
WT = 8				WT = 64			
-5		-5.0	-1.2	-5	-7.8	-5.0	-3.2
-4		-4.2	-0.6	-4	-6.3	-4.0	-2.4
-3	-10.0	-3.2	0.1	-3	-4.9	-3.0	-1.6
-2	-8.5	-2.3	0.8	-2	-3.6	-2.0	-0.8
-1	-6.7	-1.3	1.6	-1	-2.4	-1.0	0.1
0	-4.9	-0.2	2.4	0	-1.2	0.0	1.0
1	-3.2	0.8	3.3	1	-0.1	1.0	2.0
2	-1.7	1.8	4.2	2	0.9	2.0	2.9
3	-0.4	2.5	5.1	3	2.0	3.0	3.8
4	0.9	3.8	6.0	4	3.1	4.0	4.8
5	2.0	4.8	6.9	5	4.1	5.0	5.8

Table 4. P_D as a function of TW and TSNR.

Correlator - Constant Signal

Input SNR (dB)	TSNR P_D (90%)	TSNR P_D (50%)	TSNR P_D (10%)	Input SNR (dB)	TSNR P_D (90%)	TSNR P_D (50%)	TSNR P_D (10%)
WT = 2				WT = 16			
-5		-4.0	0.6	-5		-5.1	-2.1
-4		-3.6	1.0	-4	-9.3	-4.1	-1.5
-3		-3.0	1.4	-3	-7.2	-3.1	-0.8
-2	-9.9	-2.3	2.0	-2	-5.3	-2.1	-0.1
-1	-8.8	-1.4	2.6	-1	-3.6	-1.1	0.7
0	-7.4	-0.4	3.2	0	-2.1	0.0	1.5
1	-5.5	0.6	3.9	1	-0.7	1.0	2.3
2	-3.6	1.7	4.6	2	0.6	2.0	3.1
3	-1.6	2.8	5.3	3	1.7	3.0	4.0
4	0.2	3.8	6.1	4	2.9	4.0	4.9
5	1.8	4.8	6.9	5	4.1	5.0	5.8
WT = 4				WT = 32			
-5		-4.7	-0.4	-5	-9.3	-5.1	-2.8
-4		-4.0	0.1	-4	-7.3	-4.1	-2.1
-3		-3.2	0.6	-3	-5.6	-3.0	-1.4
-2	-8.9	-2.2	1.2	-2	-4.1	-2.0	-0.6
-1	-7.2	-1.2	1.9	-1	-2.7	-1.0	0.2
0	-5.2	-0.2	2.6	0	-1.4	0.0	1.1
1	-3.2	0.8	3.3	1	-0.2	1.0	1.9
2	-1.4	1.9	4.1	2	1.0	2.0	2.8
3	0.2	2.9	4.8	3	2.2	3.0	3.7
4	1.6	3.9	5.6	4	3.3	4.0	4.7
5	3.0	4.9	6.5	5	4.3	5.0	5.6
WT = 8				WT = 64			
-5		-5.0	-1.4	-5	-7.7	-5.0	-3.4
-4		-4.1	-0.8	-4	-6.1	-4.0	-2.6
-3	-9.2	-3.1	-0.2	-3	-4.7	-3.0	-1.8
-2	-7.2	-2.1	0.5	-2	-3.4	-2.0	-1.0
-1	-5.2	-1.1	1.2	-1	-2.2	-1.0	-0.1
0	-3.3	-0.1	1.9	0	-1.0	0.0	0.8
1	-1.7	0.9	2.7	1	0.2	1.0	1.7
2	-0.2	1.9	3.5	2	1.3	2.0	2.6
3	1.1	2.9	4.3	3	2.4	3.0	3.6
4	2.4	4.0	5.2	4	3.4	4.0	4.6
5	3.7	5.0	6.1	5	4.4	5.0	5.5

Table 5. P_D as a function of TW and TSNR.

Correlation Coefficient Gaussian Signal

Input SNR (dB)	TSNR P_D (90%)	TSNR P_D (50%)	TSNR P_D (10%)	Input SNR (dB)	TSNR P_D (90%)	TSNR P_D (50%)	TSNR P_D (10%)
WT = 2				WT = 16			
-5		-1.1	6.8	-5		-4.9	-0.9
-4		-0.8	7.1	-4		-3.9	-0.2
-3	-9.9	-0.4	7.6	-3	-8.7	-2.9	0.5
-2	-9.4	0.2	8.1	-2	-6.7	-1.9	1.2
-1	-8.9	0.8	8.8	-1	-5.0	-0.9	2.0
0	-8.0	1.6	9.5	0	-3.5	0.1	2.9
1	-7.2	2.4	10.2	1	-2.1	1.1	3.7
2	-6.3	3.3		2	-0.9	2.1	4.6
3	-5.2	4.3		3	0.3	3.1	5.5
4	-4.0	5.3		4	1.5	4.1	6.4
5	-2.6	6.3		5	2.6	5.1	7.4
WT = 4				WT = 32			
-5		-3.3	2.9	-5		-5.0	-1.9
-4		-2.8	3.3	-4	-8.2	-4.0	-1.2
-3		-2.2	3.9	-3	-6.4	-3.0	-0.4
-2		-1.4	4.5	-2	-4.9	-2.0	0.3
-1	-8.9	-0.5	5.2	-1	-3.6	-1.0	1.2
0	-7.6	0.5	6.0	0	-2.3	0.0	2.1
1	-6.1	1.5	6.8	1	-1.1	1.0	2.9
2	-4.5	2.5	7.6	2	0.1	2.0	3.9
3	-3.0	3.5	8.5	3	1.2	3.0	4.8
4	-1.5	4.5	9.4	4	2.3	4.0	5.7
5	-0.1	5.5		5	3.4	5.0	6.7
WT = 8				WT = 64			
-5		-4.5	0.6	-5	-8.2	-5.0	-2.7
-4		-3.7	1.2	-4	-6.6	-4.0	-2.0
-3		-2.8	1.8	-3	-5.3	-3.0	-1.2
-2	-9.0	-1.8	2.5	-2	-4.0	-2.0	-0.3
-1	-7.2	-0.8	3.3	-1	-2.7	-1.0	0.6
0	-5.4	0.2	4.0	0	-1.6	0.0	1.5
1	-3.7	1.2	4.9	1	-0.4	1.0	2.4
2	-2.2	2.2	5.7	2	0.7	2.0	3.3
3	-0.9	3.2	6.6	3	1.7	3.0	4.3
4	0.4	4.2	7.6	4	2.8	4.0	5.2
5	1.6	5.2	8.5	5	3.8	5.0	6.2

Table 6. P_D as a function of TW and TSNR.

Correlation Coefficient – Constant Signal

Input SNR (dB)	TSNR P_D (90%)	TSNR P_D (50%)	TSNR P_D (10%)	Input SNR (dB)	TSNR P_D (90%)	TSNR P_D (50%)	TSNR P_D (10%)
WT = 2				WT = 16			
-5		-1.3	6.8	-5		-4.9	-1.0
-4		-1.0	7.1	-4	-9.9	-3.9	-0.3
-3	-9.7	-0.6	7.5	-3	-7.9	-2.9	0.3
-2	-9.2	0.0	8.1	-2	-5.9	-1.9	1.1
-1	-8.5	0.8	8.7	-1	-4.2	-0.9	1.8
0	-7.4	1.7	9.4	0	-2.8	0.1	2.7
1	-5.7	2.7		1	-1.4	1.2	3.5
2	-3.9	3.8		2	-0.1	2.2	4.3
3	-2.0	4.8		3	1.1	3.2	5.2
4	-0.3	5.9		4	2.2	4.2	6.1
5	1.3	7.0		5	3.4	5.2	7.1
WT = 4				WT = 32			
-5		-3.4	2.7	-5	-9.8	-5.0	-2.0
-4		-2.9	3.2	-4	-7.8	-4.1	-1.3
-3		-2.2	3.7	-3	-6.1	-3.0	-0.6
-2	-9.4	-1.3	4.4	-2	-4.6	-1.9	0.2
-1	-7.8	-0.3	5.0	-1	-3.2	-0.9	1.0
0	-6.0	0.7	5.8	0	-1.9	0.1	1.9
1	-4.1	1.8	6.5	1	-0.7	1.1	2.7
2	-2.3	2.8	7.3	2	0.5	2.1	3.6
3	-0.7	3.9	8.2	3	1.6	3.1	4.5
4	0.8	4.9	9.1	4	2.7	4.1	5.5
5	2.1	5.9	10.0	5	3.8	5.1	6.4
WT = 8				WT = 64			
-5		-4.5	0.5	-5	-8.1	-5.0	-2.9
-4		-3.7	1.1	-4	-6.5	-4.0	-2.1
-3	-9.9	-2.7	1.7	-3	-4.7	-3.0	-1.3
-2	-8.0	-1.7	2.4	-2	-3.8	-2.0	-0.5
-1	-5.9	-0.7	3.1	-1	-2.5	-1.0	0.4
0	-4.1	0.3	3.8	0	-1.3	0.0	1.3
1	-2.4	1.4	4.6	1	-0.2	1.0	2.2
2	-1.0	2.4	5.5	2	0.9	2.0	3.1
3	0.4	3.4	6.4	3	2.0	3.0	4.1
4	1.6	4.4	7.2	4	3.1	4.0	5.0
5	2.8	5.4	8.1	5	4.1	5.0	6.0

Table 7. P_D as a function of TW and TSNR.

Coherence Detector – Gaussian Signal

Input SNR (dB)	TSNR P_D (90%)	TSNR P_D (50%)	TSNR P_D (10%)	Input SNR (dB)	TSNR P_D (90%)	TSNR P_D (50%)	TSNR P_D (10%)
WT = 2				WT = 16			
-5	-3.0	4.3		-5	-8.2	-3.5	-0.2
-4	-2.8	4.4		-4	-7.3	-2.9	0.4
-3	-2.7	4.7		-3	-6.3	-2.1	1.0
-2	-2.5	4.9		-2	-5.2	-1.3	1.7
-1	-2.2	5.4		-1	-4.0	-0.4	2.4
0	-1.8	5.8		0	-2.8	0.5	3.2
1	-1.3	6.4		1	-1.6	1.5	4.0
2	-0.7	7.0		2	-0.4	2.4	4.9
3	0.0	7.7		3	0.7	3.4	5.8
4	0.7	8.5		4	1.8	4.4	6.7
5	1.6	9.4		5	2.9	5.4	7.6
WT = 4				WT = 32			
-5	-5.8	0.0	5.1	-5	-8.1	-4.3	-1.5
-4	-5.5	0.2	5.4	-4	-6.9	-3.4	-0.9
-3	-5.1	0.6	5.8	-3	-5.6	-2.6	-0.2
-2	-4.7	1.1	6.3	-2	-4.4	-1.6	0.6
-1	-4.2	1.7	6.9	-1	-3.2	-0.7	1.4
0	-3.5	2.3	7.5	0	-2.0	0.2	2.2
1	-2.6	3.1	8.2	1	-0.9	1.2	3.1
2	-1.7	3.9	9.0	2	0.2	2.2	4.0
3	-0.7	4.8	9.8	3	1.3	3.2	4.9
4	0.3	5.6		4	2.4	4.2	5.8
5	1.4	6.6		5	3.5	5.2	6.8
WT = 8				WT = 64			
-5	-7.4	-2.3	1.9	-5	-7.5	-4.6	-2.5
-4	-6.9	-1.8	2.3	-4	-6.2	-3.7	-1.8
-3	-6.4	-1.2	2.8	-3	-4.9	-2.8	-1.0
-2	-5.6	-0.5	3.4	-2	-3.8	-1.8	-0.2
-1	-4.6	0.3	4.1	-1	-2.6	-0.9	0.7
0	-3.6	1.1	4.8	0	-1.4	0.1	1.6
1	-2.4	2.0	5.5	1	-0.3	1.1	2.5
2	-1.3	2.9	6.3	2	0.7	2.1	3.4
3	-0.1	3.8	7.2	3	1.8	3.1	4.3
4	1.0	4.7	8.1	4	2.8	4.1	5.3
5	2.1	5.7	9.0	5	3.9	5.1	6.2

Table 8. P_D as a function of TW and TSNR.

Coherence Detector – Constant Signal

Input SNR (dB)	TSNR P_D (90%)	TSNR P_D (50%)	TSNR P_D (10%)	Input SNR (dB)	TSNR P_D (90%)	TSNR P_D (50%)	TSNR P_D (10%)
WT = 2				WT = 16			
-5	-3.0	4.2		-5	-8.1	-3.5	-0.3
-4	-3.0	4.3		-4	-7.1	-2.9	0.3
-3	-2.7	4.6		-3	-6.0	-2.1	0.9
-2	-2.5	5.0		-2	-4.7	-1.2	1.5
-1	-2.0	5.3		-1	-3.4	-0.3	2.3
0	-1.4	5.9		0	-2.2	0.6	3.0
1	-0.6	6.6		1	-0.9	1.5	3.8
2	0.3	7.3		2	0.2	2.5	4.6
3	1.4	8.1		3	1.4	3.5	5.5
4	2.5	9.0		4	2.5	4.4	6.4
5	3.7	9.9		5	3.6	5.4	7.3
WT = 4				WT = 32			
-5	-5.9	-0.2	5.2	-5	-8.0	-4.3	-1.6
-4	-5.6	0.2	5.5	-4	-6.7	-3.4	-1.0
-3	-5.1	0.5	5.9	-3	-5.4	-2.5	-0.3
-2	-4.5	1.1	6.3	-2	-4.1	-1.6	0.4
-1	-3.9	1.7	6.8	-1	-2.9	-0.7	1.2
0	-2.8	2.5	7.5	0	-1.7	0.3	2.0
1	-1.7	3.3	8.1	1	-0.5	1.2	2.9
2	-0.5	4.1	8.9	2	0.6	2.2	3.8
3	0.6	5.1	9.6	3	1.7	3.2	4.7
4	1.9	6.0		4	2.8	4.2	5.6
5	3.0	7.0		5	3.9	5.2	6.5
WT = 8				WT = 64			
-5	-7.3	-2.3	1.8	-5	-7.4	-4.6	-2.6
-4	-6.8	-1.8	2.2	-4	-6.1	-3.7	-1.9
-3	-6.0	-1.2	2.7	-3	-4.8	-2.8	-1.1
-2	-5.1	-0.5	3.3	-2	-3.6	-1.8	-0.3
-1	-3.9	0.3	3.9	-1	-2.4	-0.9	0.5
0	-2.7	1.1	4.6	0	-1.2	0.1	1.4
1	-1.5	2.1	5.3	1	-0.1	1.1	2.3
2	-0.3	3.0	6.1	2	1.0	2.1	3.2
3	1.0	3.9	6.9	3	2.1	3.1	4.1
4	2.1	4.9	7.8	4	3.1	4.1	5.1
5	3.3	5.9	8.7	5	4.2	5.1	6.0

Table 9. P_D as a function of TW and TSNR.

RESULTS AND DISCUSSION

The primary results are contained in figures 2, 3, 4, and 5. These show false-alarm probability as a function of threshold signal-to-noise ratio.

Note that this is bin false-alarm probability, or the probability of a false alarm on a single "look." Since a practical system is likely to have several thousand opportunities for a false alarm (or several thousand "looks") in a reasonably short time period, the system false-alarm rate per day may be several orders of magnitude greater. Thus, bin false-alarm probabilities greater than about 10^{-4} are probably unacceptable. The important data in figures 2, 3, 4, and 5 are between $P_f = 10^{-4}$ and $P_f = 10^{-8}$. The remaining discussion will address only this region.

Several points in these figures are interesting to note.

In figure 2, it can be seen that, for a given false-alarm probability, the curves for various WT values are separated by about 1.5 dB in the large WT cases. This agrees with the general rule that the integration gain of a detection is 5 log (WT). However, for small WT values, the separation of the curves increases to about 2.5 dB. This is because the 5 log (WT) rule is based on an application of the central limit theorem, which breaks down for small WT. In some cases, this can lead to a difference of 3 or 4 dB in minimum detectable signal. It is likely that this difference is sometimes noted in system evaluations as "processing loss" or "operator loss."

It is interesting to note that the curves in figure 3 very closely overlay those in figure 2, with a shift in WT; eg, the curve for WT = 1 in figure 3 overlays the curve for WT = 2 in figure 2. In other words, the advantage in using a correlator over using a square law detector is a factor of 1/2 in the integration time needed to achieve a given performance level.

For large WT, the curves in figures 3, 4, and 5 nearly overlay. For large WT, all three of these techniques give nearly the same performance. Selection among these formulas can thus be made on the basis of considerations other than detection performance, such as ease of implementation.

For small WT, the performance in curves 4 and 5 deteriorates rapidly. In fact, curves for WT less than 8 were not plotted. This indicates that the normalized algorithms should be used only in high WT cases. In situations where short integration time is needed, the normalization should not be used.

Figures 8, 9, and 10 were extracted from figures 2, 3, 4, and 5 to facilitate interalgorithm comparisons. Figure 8 represents data from a cut along the $P_f = 10^{-8}$ axis. Threshold signal-to-noise ratio (TSNR) is plotted as a function of time-bandwidth product (WT). Here the deterioration of the normalized estimators can be clearly seen.

As was observed earlier, the square law detector provides a natural baseline to compare the other algorithms against. Only the correlator is better for all values of WT. (It should be remembered that this assumes equal signal strength in both sequences. If the

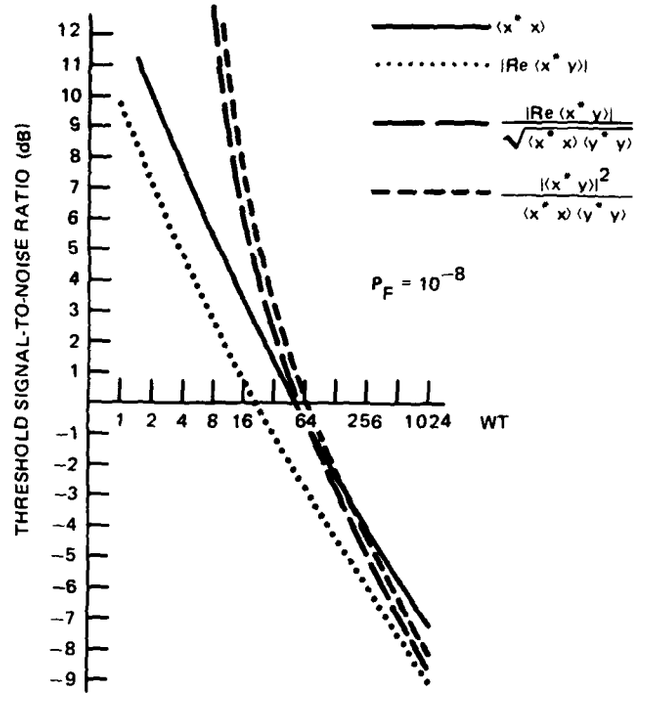

Figure 8. Threshold signal-to-noise ratio as a function of WT.

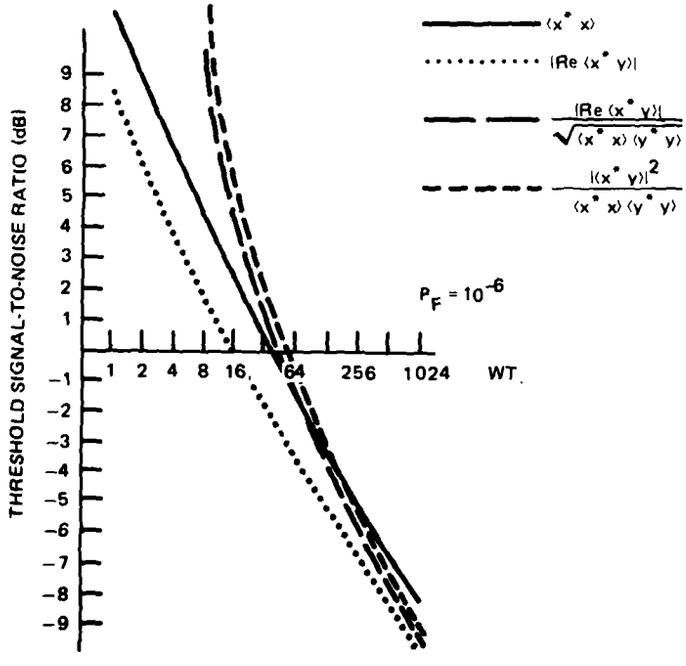

Figure 9. Threshold signal-to-noise ratio as a function of WT.

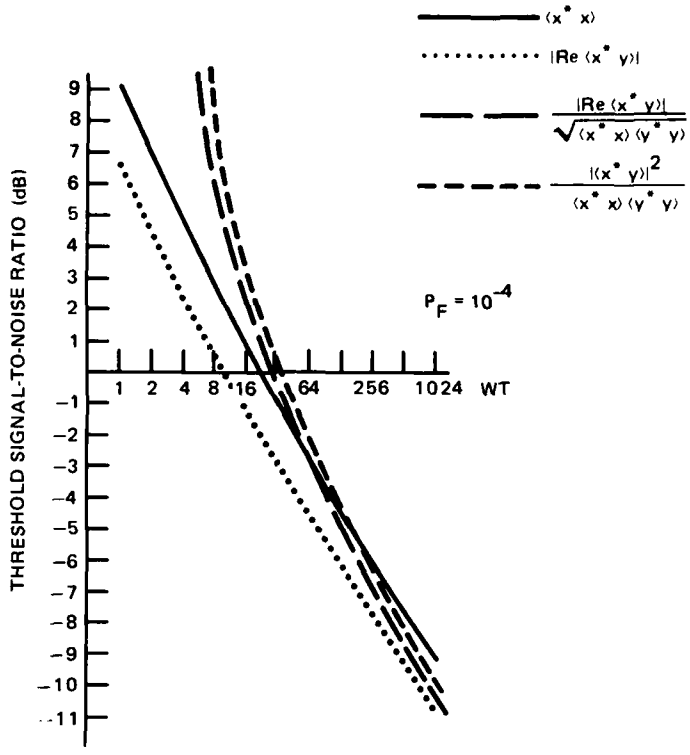

Figure 10. Threshold signal-to-noise ratio as a function of WT.

signal in one sequence falls off, it will decrease the performance of the correlator.) The normalized formulas are superior to the square law detector only for WT values greater than 64.

Figures 9 and 10 show similar data for higher false-alarm probabilities. They indicate that the results are not very sensitive to false-alarm probability, since the curves do not change very much. In general, a change in false-alarm probability of four orders of magnitude (for 10^{-8} to 10^{-4}) corresponds to a change in TSNR of about 3 dB. For $P_f = 10^{-4}$, the crossover between the square law detector and the normalized formulas has moved slightly to the left of WT = 64.

Inclusion of all of the data from the signal plus noise simulations would increase the size of this report severalfold, but without contributing much to the utility. However, tables 1 through 8 have been extracted from those simulations. They use input signal-to-noise ratio (ISNR) as the independent variable. Then, for each true input signal-to-noise ratio, they show the threshold signal-to-noise ratio at which detections would occur with a probability of 0.9, 0.5, or 0.1. This can be combined with the false-alarm information.

For example, suppose a square law detector with WT = 32 is to be used. What would it take to detect a Gaussian signal which appears at the input with a signal-to-noise ratio of 0 dB? From table 1, such a signal would be detected 10% of the time if the threshold signal-to-noise ratio were set at 1.7 dB. The probability of detection could be increased to 50% by lowering the threshold signal-to-noise ratio to −0.1 dB. To achieve a 90% probability of detection, the threshold signal-to-noise ratio would have to be lowered further to −2.5 dB.

However, from figure 2, a threshold signal-to-noise ratio of −2.5 dB corresponds to a false-alarm probability of about 3×10^{-3}, an unreasonably high value. Thus a 90% probability of detection is not reasonably achievable. A threshold signal-to-noise ratio of −0.1 dB, from the same figure, corresponds to a false-alarm probability of about 3×10^{-6}, which is reasonable. Thus a probability of detection of 50% is achievable with a false-alarm probability which may be acceptable. Again, from figure 2, a threshold signal-to-noise ratio of 1.7 dB corresponds to a false-alarm probability of less than 10^{-9}. So a probability of detection of 10% can be achieved with almost any reasonable threshold.

From these tables and figures, figures 11 through 19 were extracted. Here the vertical axis shows the input signal-to-noise ratio at which detections will occur with a prescribed probability when the detector has been set for a certain false-alarm probability. Moreover, when a second line for a given algorithm is discerned, the higher line applies to performance with a Gaussian signal. Figures 11 through 19 invite comparison with figures 8, 9, and 10. The main result is that the performance evaluation does not change greatly with modest changes in the assumptions about signal type or desired probability of detection. Thus one can obtain a fairly good estimate of the detector performance merely by using figures 2 through 5 and 8 through 10.

It should be noted that none of the above signal-to-noise ratios is equal to the recognition differential. They differ from recognition differential at least by a bandwidth correction factor. More importantly, the definition and measurement of recognition differential involve human engineering and/or system subtleties which are beyond the scope of this paper.

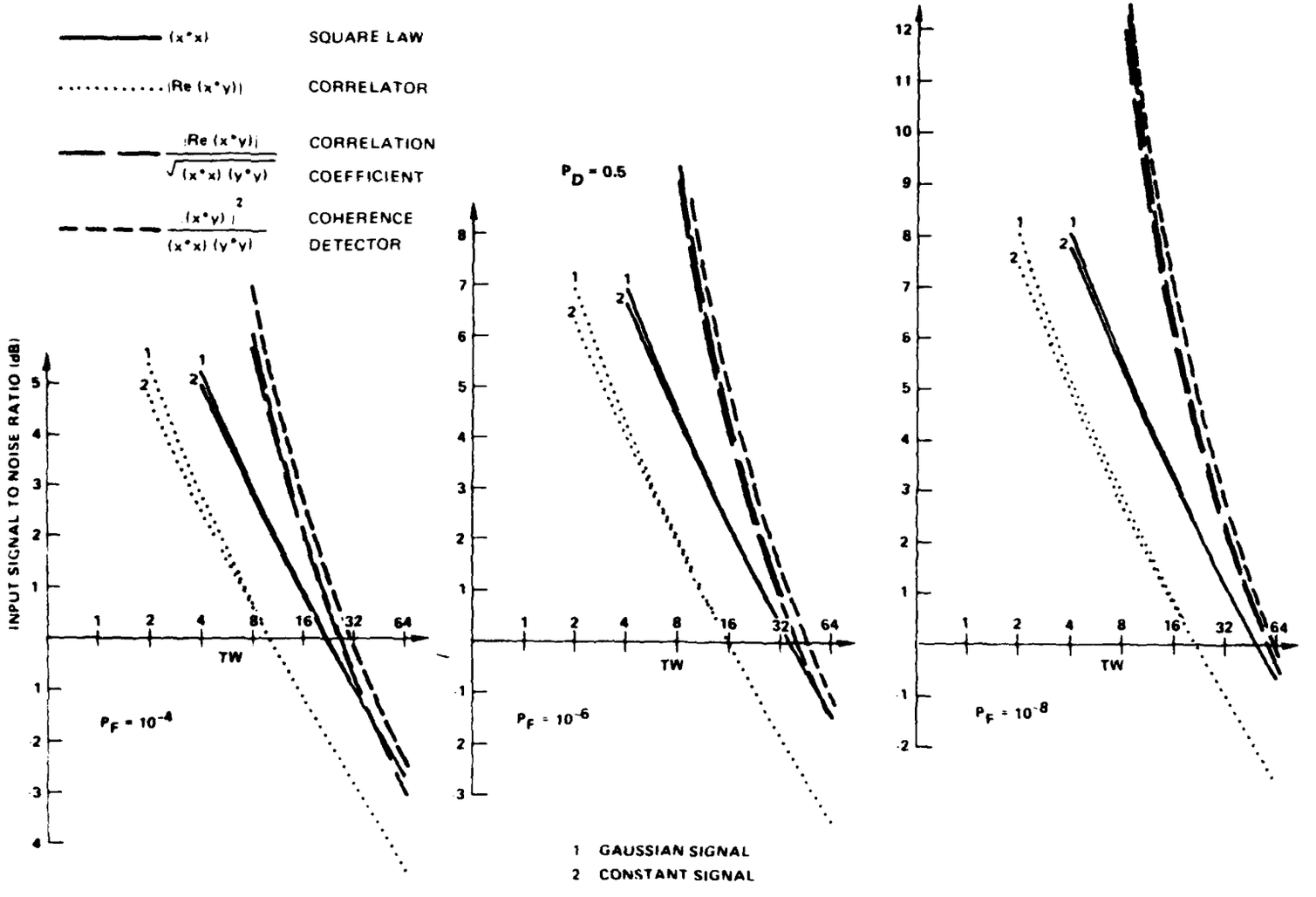

Figure 11. Algorithm performance as a function of time-bandwidth product.

Figure 12. Algorithm performance as a function of time-bandwidth product.

Figure 13. Algorithm performance as a function of time-bandwidth product.

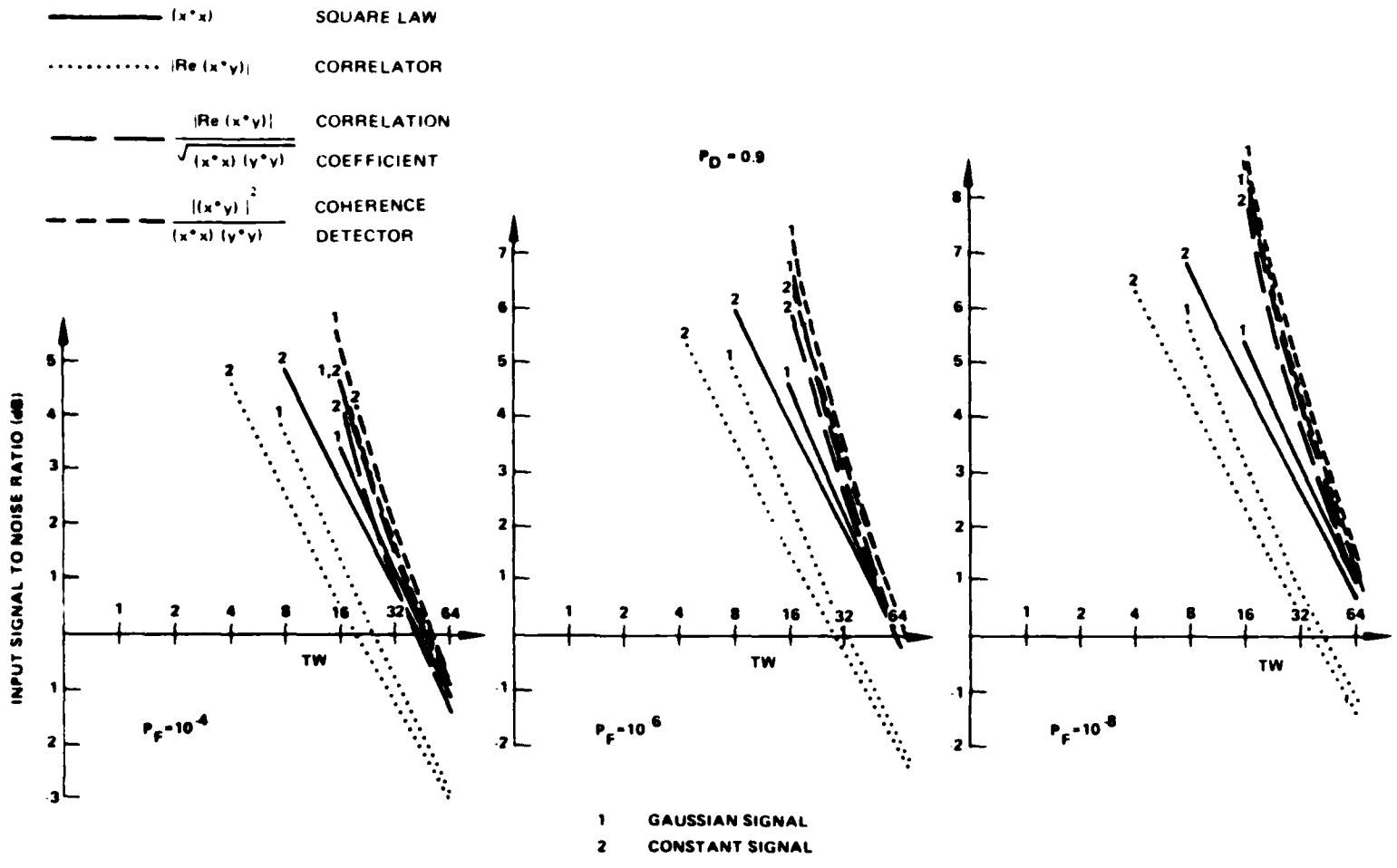

Figure 14. Algorithm performance as a function of time-bandwidth product.

Figure 15. Algorithm performance as a function of time-bandwidth product.

Figure 16. Algorithm performance as a function of time-bandwidth product.

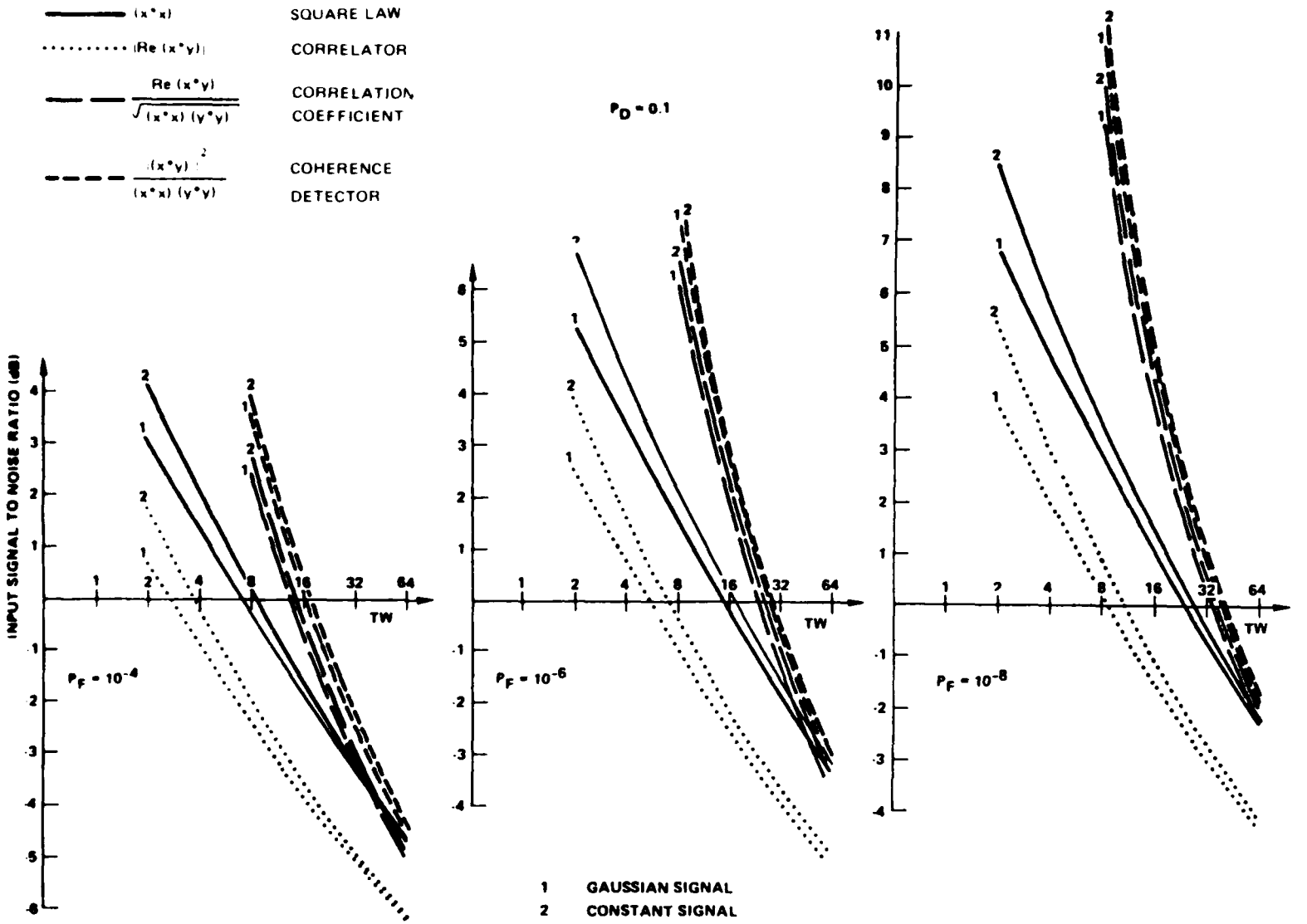

Figure 17. Algorithm performance as a function of time-bandwidth product.

Figure 18. Algorithm performance as a function of time-bandwidth product.

Figure 19. Algorithm performance as a function of time-bandwidth product.

REFERENCES

1. Van Trees, H. L., Detection, Estimation and Modulation Theory, Part I, John Wiley and Sons, Inc., 1968.

2. Mood, A. M., and F. A. Graybill, Introduction to the Theory of Statistics, McGraw-Hill, 1963.

3. Goodman, N. R., On the Joint Estimation of the Spectra, Cospectrum, and Quadrature Spectrum of a Two-Dimensional Stationary Gaussian Process, New York University, Engineering Statistics Laboratory, March 1957.